ORIGINAL ARTICLE

Investigation on magnetic and flow field in magnetorheological jet machining

Zhe Lv[1] · Rongguo Hou[1] · Guoyong Zhao[1]

Abstract

The instability and spreading out of jet flow outside the focusing tube involved in abrasive waterjet machining can be prevented by using magnetorheological (MR) fluid. The collimated and coherent MR jet in the presence of external axial magnetic field is potential to give a preferable erosion footprint and processing performance. In this research, a magnetic generator was developed and installed on an abrasive waterjet machining system to conduct MR jet erosion experiments on alumina. The induced magnetic field and jet flow field were numerically analyzed to evaluate their effects on material removal. The results indicated that the magnetic flux density increases with an increment of excitation current. The concentration of jet flow can be significantly enhanced by applying external magnetic field, and the velocity attenuation along the flowing direction due to the jet diffusion is restrained. The experimental results indicated that the range of crater is relatively smaller, and the erosion depth is larger when applying magnetic field, which can verify the validity of simulation results.

Keywords Computational fluid dynamics · Abrasive waterjet · Impact fluid field · Magnetic field

1 Introduction

Micro-abrasive waterjet has been widely used in the processing of hard-brittle materials which is difficult for traditional machining methods. The successive erosions of discrete fine abrasive particles can effectively avoid fractures on the workpiece surface. Moreover, the heat generated during the material removal can be easily removed by the water, which can prevent the surface from thermal damage. Principles of abrasive waterjet such as jet flow structure, mixing procedure, and impact dynamics of particles have been investigated by many researchers. The abrasive waterjet ejected out from the focusing tube is surrounded by droplets and solid particles [1]. The jet is oscillated in axial and radial directions. The oscillations turn into strong perturbations and disturb the continuity of the abrasive waterjet [2]. The mass flow rate of particles has an effect on the diameter of the jet. High abrasive mass flow rate can lead to the shortening of steady zone of the jet and a severe increase of jet diameter [3].

In abrasive waterjet machining, the jet flow outside the focusing tube has a strong diffusing characteristic due to its high-velocity [4]. The outer layer of the jet fluid shows intensive turbulence under the high-velocity gradient towards the surrounding ambient air [5]. The diffusion of jet will leads to significant attenuation on kinetic energy of abrasive particles. Magnetorheological fluid is a mixture of high magnetic permeability powders and non-conductive base liquid. Under strong magnetic field, magneto rheological fluid turns to Bingham body with high viscosity and shear yield strength [6]. Kordonski et al. [7] firstly used magneto rheological fluid with the addition of high-hardness particles in surface finishing. Bingham fluid under external magnetic field is driven by a rotating spindle and can well fit the surface shape [8]. Material can be removed through scratching of micro-hard particles constrained in fluid [9]. Jha and Jain [10] used magneto rheological abrasive flow in finishing of internal geometries of hard materials. The arrangements of carbonyl iron particles and silicon carbide particles were analyzed. The force exerted on abrasive particle, and the surface roughness is modeled. Wang et al. [11] investigated the planarization process using magnetorheological fluid. The results indicated that the effects of carbonyl iron particles concentration on polishing force and surface roughness are significant. Wang et al. [12] utilized ultrasonic-magnetorheological finishing

---

✉ Zhe Lv
  lzjslyz@126.com

1 School of Mechanical Engineering, Shandong University of Technology, Zibo 255000, China

method on quartz silica. The polishing head vibrated at longitude direction to apply additional force on magneto rheological fluid medium. The impact force of abrasive particle was modeled, and the experimental results showed that the material removal was increased by the compound effect of magnetic field and ultrasonic vibration.

In order to stabilize the jet flow outside the focusing tube, Tricard and Kordonski [13] proposed magnetorheological jet machining. By using magnetorheological fluid instead of pure water, the ambient disturbance and the spreading out of jet can be effectively avoided when applying axial magnetic field adjacent to the focusing tube. High apparent viscosity and shear strength of magnetorheological jet will suppress air entrainment and intensive turbulence at the outer layer. The experimental results indicated that the removal function of the collimated and coherent jet is stable and suitable for the processing of complex configurations. The erosion ability of magnetorheological jet is closely relevant to its flow characteristics such as pressure and velocity distributions. However, few literatures have been concerned about the flow field of MR jet.

In present research, flow characteristics and erosion performance of magnetorheological jet were investigated by establishing numerical models. A magnetic field generating apparatus was developed and mounted on the abrasive waterjet machining system. The distribution of magnetic flux was numerically calculated. Then, the magnetorheological jet flow was simulated in the presence of magnetic field generated by the excitation coil. Finally, experiments were conducted for demonstrating the feasibility of this processing method.

2 Modeling

The equipment implied for generating magnetic field mainly consists of a direct-current power supply, a relay, a current regulator, and a coil set. Appropriate amount of current is exerted on the coil to generate the defined intensity of magnetic field. Therefore, the current carrying coil is modeled in electromagnetic module of ANSYS 15 to evaluate the magnetic field parameters. The schematic of the coil set and focusing tube is shown in Fig. 1. The coil is wound by polyester enameled copper wire with a diameter of 0.8 mm. The outer and inner radiuses of the coil set are 40 mm and 20 mm, respectively. The length of the coil is 80 mm, and the number of turns is 2000. The output of current regulator is ranged in 0–1.8 A. The inner and outer diameters of the stainless steel focusing tube are 1 mm and 8 mm, respectively.

A two-dimensional axisymmetric model is suitable for the approximation of coil set and saves computation resources. An eight-node magnetic vector element (PLANE 53) is implemented for all the computational regions. The finite element model is shown in Fig. 2. The size of the coil zone is
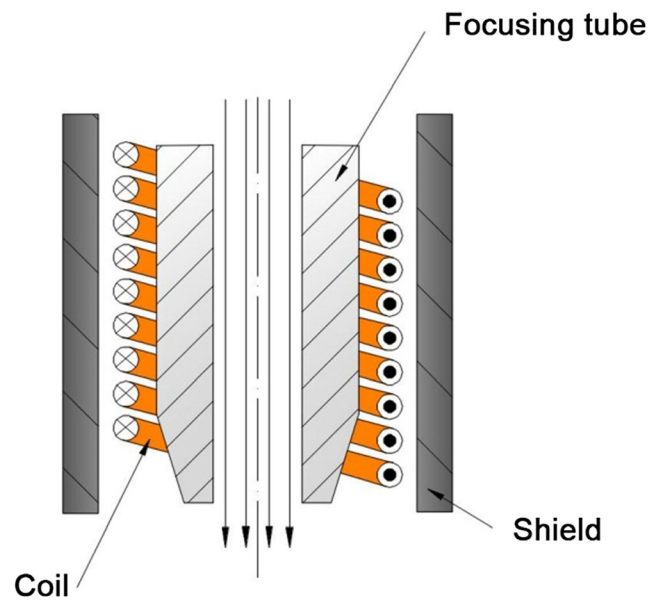

Fig. 1 Schematic of coil set and focusing tube

corresponding to the actual dimensions. The length, turn number, and filling factor of the coil are set in the real constants of the elements. Excitation current density is calculated corresponding to the physical conditions and exerted on the elements of coil. The infinite far field surface is applied on the outer boundary of the ambient air. The magnetic permeability of air is $4\pi \times 10^{-7}$ H/m, and the relative permeability is 1. B-H curves of the copper alloy and stainless steel are imported. Flux parallel boundary condition is applied on the inner surface of focusing tube. The solution of electromagnetic equations is obtained by introducing magnetic vector potential and electric scalar potential functions.

The coupling between the fluid flow field and the magnetic field can be understood on the basis of two fundamental effects: the induction of electric current due to the movement of conducting material in a magnetic field, and the effect of Lorentz force as the result of electric current and magnetic field interaction. In general, the induced electric current and the Lorentz force tend to oppose the mechanisms that create them. Movements that lead to electromagnetic induction are therefore systematically braked by the resulting Lorentz force. Electric induction can also occur in the presence of a time-varying magnetic field. The effect is the stirring of fluid movement by the Lorentz force. Electromagnetic fields can be described by Maxwell's equations [14].

In studying the interaction between flow field and electromagnetic field, it is critical to know the current density due to induction. Generally, two approaches may be used to evaluate the current density. One is through the solution of a magnetic induction equation. The magnetic induction equation is derived from Ohm's law and Maxwell's equation. The equation provides the coupling between the flow field and the magnetic field [15]:

Fig. 2 Mesh model of the excitation coil
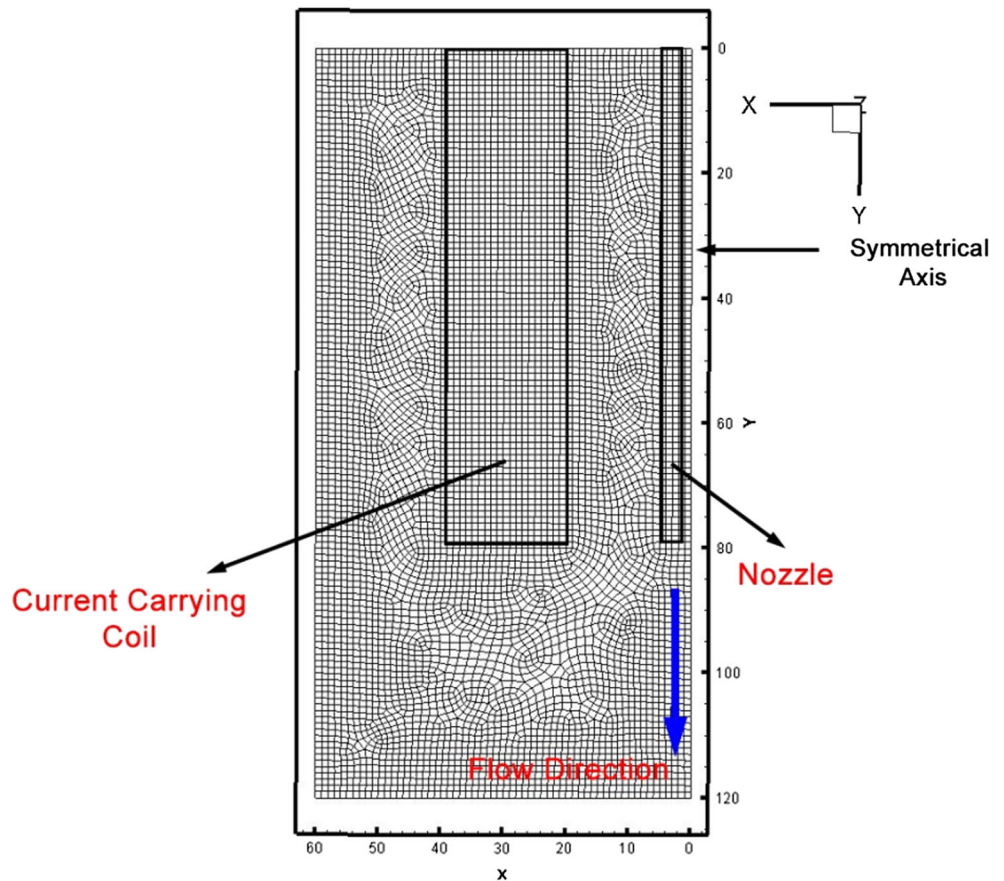
$$\frac{\partial B}{\partial t} + (V \cdot \nabla)B = \frac{1}{\mu\sigma}\nabla^2 B + (B \cdot \nabla)V \qquad (1)$$

where B is the magnetic induction intensity, V is the fluid velocity, μ is the magnetic permeability, and σ is the electrical conductivity. From the solved magnetic field, the current density can be calculated using Ampere's relation as:

$$J = \frac{1}{\mu}\nabla \times B \qquad (2)$$

where J is the current density. Generally, the magnetic field in a MHD problem can be decomposed into the externally imposed field and the induced field due to fluid motion. Only the induced field must be solved.

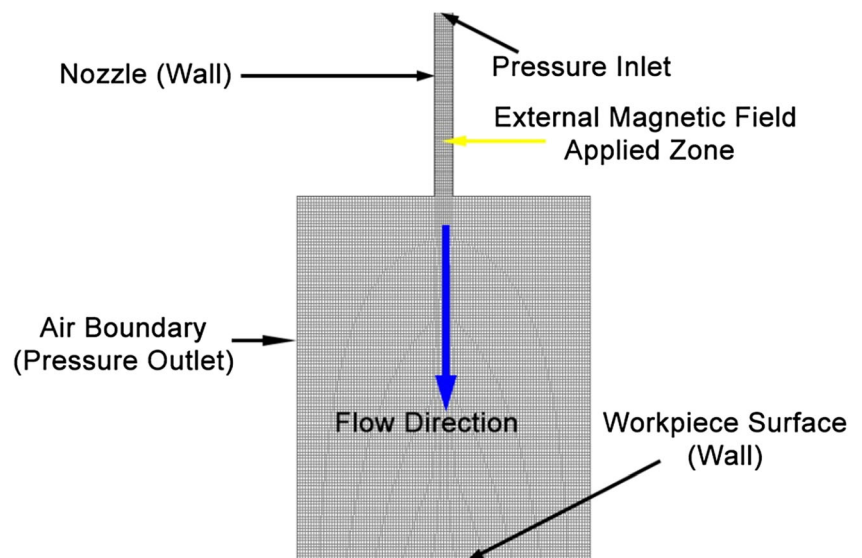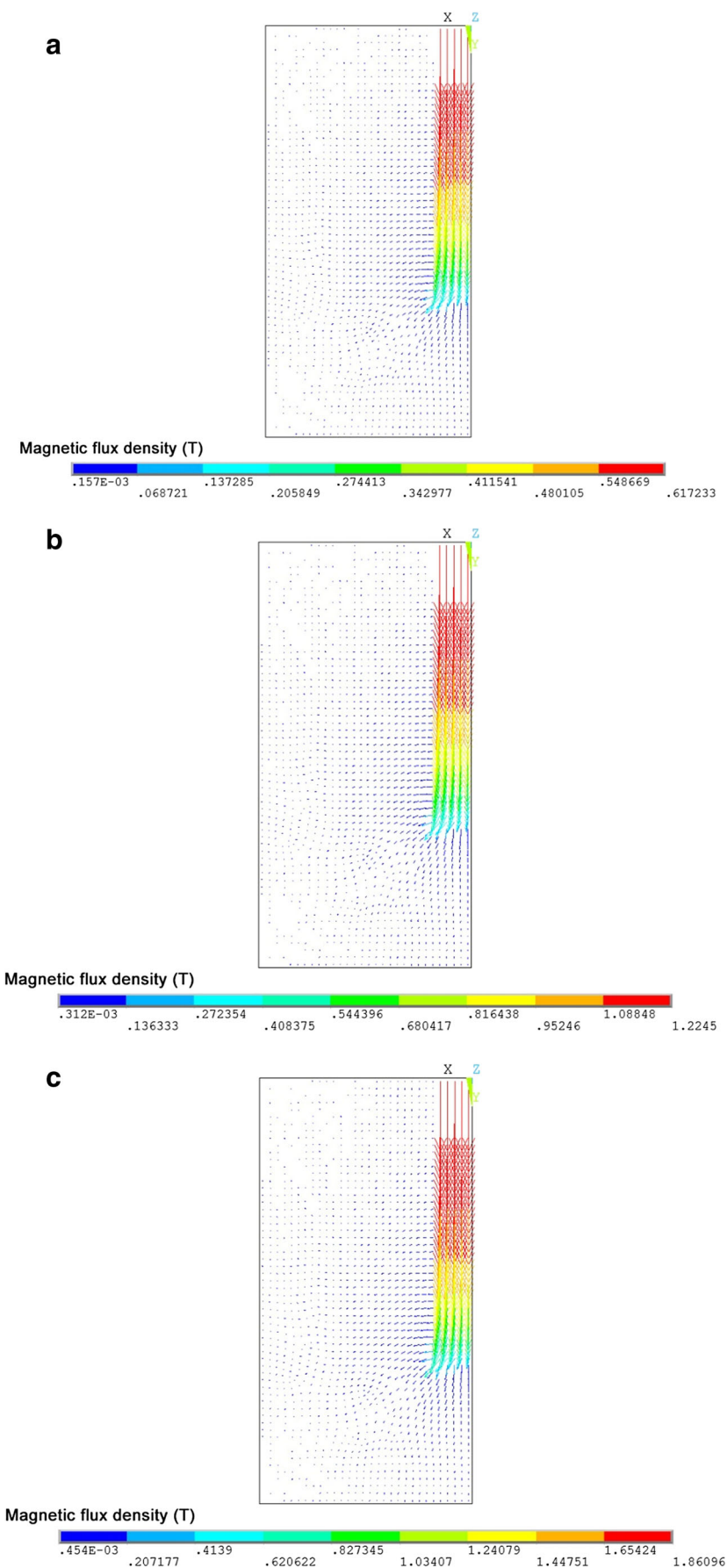**Fig. 3** Computational model of the MR jet fluid field

Fig. 4 Vector plots of magnetic flux densities of under different current magnitudes (pressure = 10 MPa). **a** Current = 0.5 A. **b** Current = 1 A. **c** Current = 1.5 A
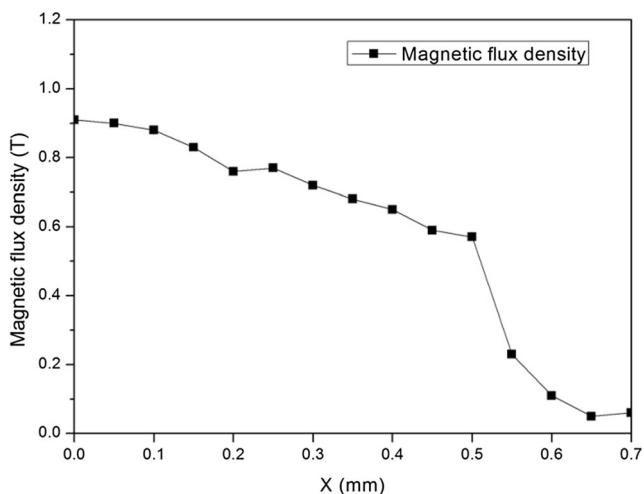
Fig. 5 Magnetic flux density distribution at the focusing tube outlet (current = 1.5 A, pressure = 10 MPa)

The Lorentz force can therefore be introduced into momentum equation of fluid:

$$\frac{\partial(\rho V)}{\partial t} + (\rho V \cdot \nabla)V = -\nabla p + \nabla \cdot (\eta \nabla V) + \rho g + F_s + J \times B \qquad (3)$$

where p is pressure, and F_s is the surface tension. η is the dynamic viscosity.

The geometrical model of computational flow field is shown in Fig. 3. The Eulerian model is implemented considering the multiphase nature of the fluid. Focusing tube is set as the pressure inlet with the pressure value ranging from 10 to 30 MPa, and outer boundary of the air is set as the pressure outlet with standard atmosphere. K-ε model is adopted to evaluate the turbulent flow characteristics. Totally 13,900 quadrilateral mesh cells are generated for the whole geometry which is separated into several regions. Mesh density has been adapted to assure the computation accuracy and take the operation efficiency into consideration at the same time.

The external magnetic field calculated from the above section is applied on the jet flow region. Magnetic fluid is composed of water, iron carbonyl powders, and dispersant. The material properties of the magnetic fluid such as electrical conductivity and magnetic permeability are set to complement the MHD cell zone conditions. Insulating wall boundary condition is set on the workpiece surface. The magnetic induction and fluid momentum equations were solved by using first-order upwind discretizing method.

3 Simulation results and discussions

The magnetic field excited by the current carrying coil is shown in Fig. 4. It can be found that the magnetic flux density

is obviously higher at central region of the field. The density of magnetic lines at outer region is relatively lower. The stainless focusing tube takes the effect of core to concentrate the magnetic lines. It can be also drawn that the magnetic flux density significantly increases with an increment of excitation current. Figure 5 illustrates magnetic flux density at the outlet of the focusing tube along the radial axis. It can be found that the magnetic flux density at the centerline is 0.91 T and decreases at the periphery region.

The velocity distribution of the fluid phase outside the focusing tube is shown in Fig. 6. It can be clearly found that the diameter of the jet decreases with an increase of magnetic induction. The result indicates that the concentration of jet flow can be significantly enhanced by applying external magnetic field. Moreover, it can be observed that the axial velocity of the jet fluid is higher when applying external magnetic field. The maximum velocity value is 155 m/s when exerting current of 1.5 A on the coil. Moreover, the velocity attenuation along the flowing direction due to the jet diffusion is restrained.

The velocity contours of jet flow fields under different pressures are shown in Fig. 7. The pressure has a strong influence on fluid velocity magnitude, which can be described by Bernoulli's equation. It can be drawn that the velocity magnitude increases with an increment of pressure. However, due to the intensive turbulence, the diffusion is enhanced and the spreading of jet is significant under higher pressure.

4 Verification experiment

4.1 Experimental conditions

The magnetic field generating apparatus was shown in Fig. 8. It is comprised of a DC output, an electric relay, a current regulator, and a coil set. The intensity of magnetic field can be adjusted by regulating the current magnitude excited on the coil. The coil set was mounted surrounding the focusing tube and the mixing tube of abrasive waterjet machining system. Magnetorheological fluid was pressurized and transported to the focusing tube. After mixing with abrasive particles in the mixing chamber, a collimated jet was ejected out under the magnetization by coil set and impacted on the workpiece surface.

Erosion experiments were conducted using the developed setup. Alumina specimens with the sizes of 10 mm × 10 mm were used as workpieces. Material of abrasive is chosen as silicon carbide and the screen mesh number is 1200#. Mass fraction of the iron carbonyl powders in MR fluid is 5%. The processed surface was measured by using a microscope after ultrasonic cleaning. Some detailed settings of experiments are detailed in Table 1.

4.2 Experimental results and discussions

The surface topologies of the eroded surfaces are shown in Fig. 9. Blue region of the contour represents the material removal induced by the erosion. It can be found that the range of crater is relatively smaller, which can be attributed to the superior concentration of coherent magnetorheological jet. The maximum erosion depth is greater when applying magnetic field. This is due to the decrease of energy loss caused by the air drag. The result indicated that the magnetorheological jet has a better removal capacity and controllability on erosion footprint.

Figure 10 illustrates the variation of erosion depth with the increase of exerting current amplitude. The erosion rate of abrasive waterjet is strongly dependent on the impingement velocity of the abrasive particles, which can be expressed as [16]:

$$R = \sum_{p=1}^{N} cm_p f(\alpha) v_p^b$$

where N is the number of particles, m_p is the mass flow rate of particles, c is a coefficient depending on target and abrasive material properties, $f(\alpha)$ is a function of impact
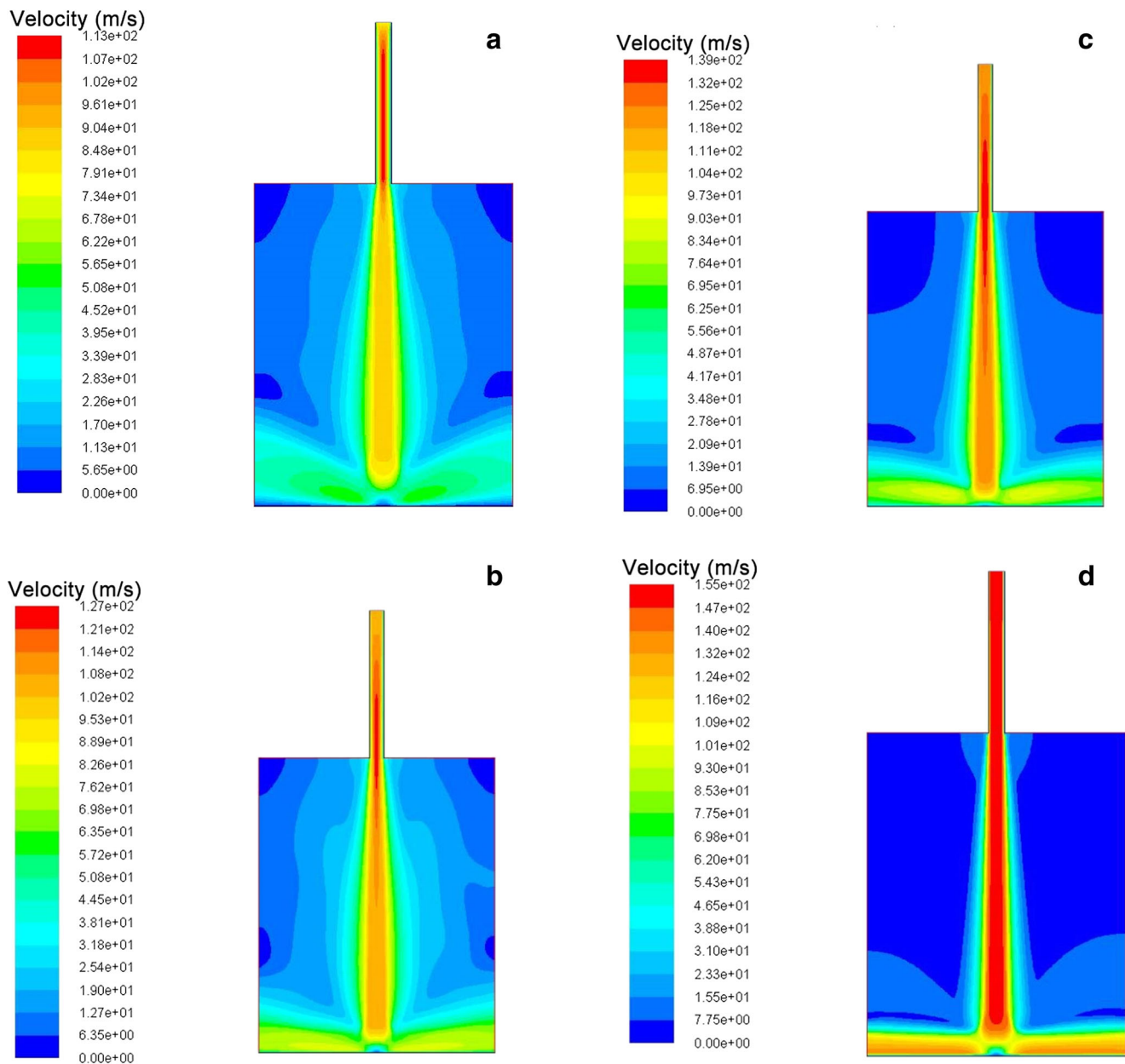

Fig. 6 Velocity distributions of the MR jet flows under different excitation currents (pressure = 10 MPa). **a** Current = 0 A. **b** Current = 0.5 A. **c** Current = 1 A. **d** Current = 1.5 A
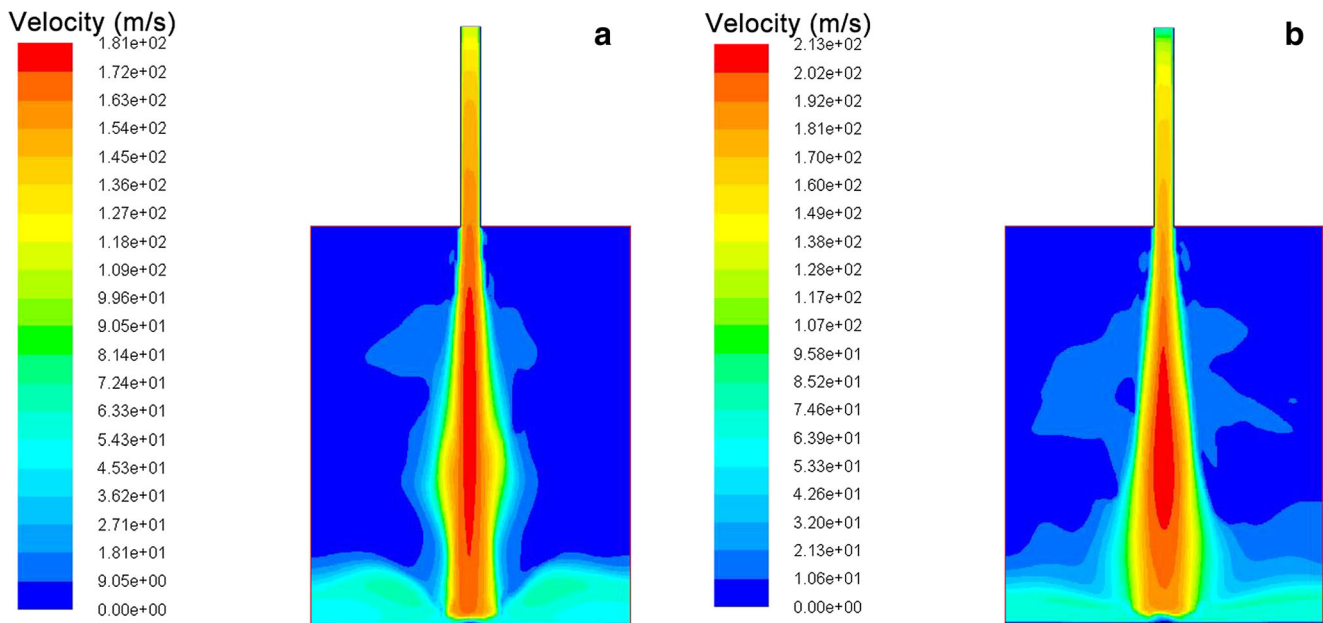
Fig. 7 Velocity distributions of the MR jet flows under different pressures (current = 1.5 A). **a** Pressure = 20 MPa. **b** Pressure = 30 MPa

angle, v_p is the particle velocity, and b is the exponent relevant to particle velocity. The particle velocity of abrasive water jet is affected by the severe disturbance induced by the air drag. Compared with the previous studies [17, 18], the erosion depth of abrasive waterjet under the same operating condition is 35% lower than that of MR jet under 0.5 A current. The increase of erosion depth of MR jet under magnetic field can be attributed to the higher impingement velocity of abrasive particles. It can be also found that the erosion depth increases with an increment of magnetic induction, which can be attributed to the improved convergence of MR jet. The result coincides with simulation result that the concentration of jet flow can be significantly enhanced by applying external magnetic field.

Fig. 8 Magnetic field generating apparatus and abrasive waterjet machining system

5 Conclusions

This paper aims to investigate the flow characteristics of magnetorheological jet under external magnetic field. Simulations and verification experiments were conducted for evaluating the erosion performance of MR jet. Some main findings are as following:

(1) The magnetic flux density excited by the current coil is higher at central region of the field and increases with an increment of excitation current.
(2) The concentration of jet flow can is enhanced, and the velocity attenuation is restrained under external magnetic field.
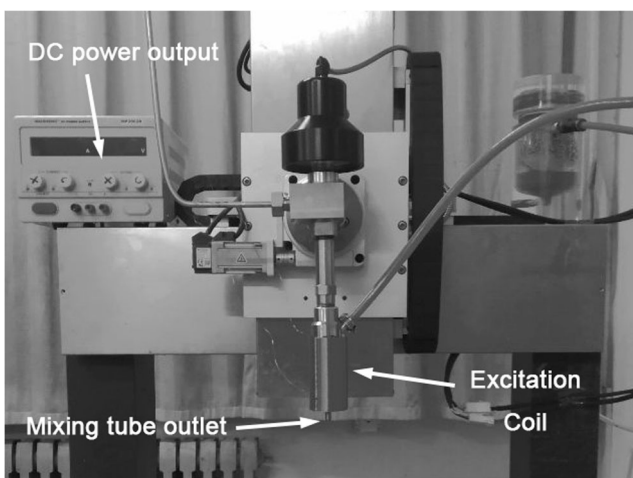(3) The range of crater is relatively smaller, and the erosion depth is larger when exerting current.

Table 1 Experimental parameters

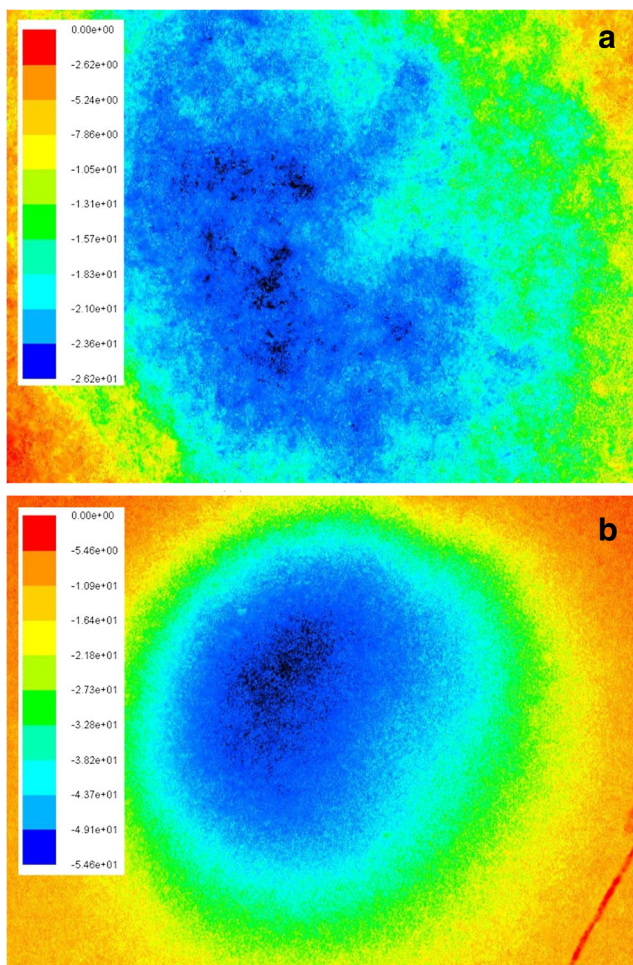| Parameters	
Excitation current (A)	0–1.5
Number of turns in coil	2000
Inner radius of coil (mm)	20
Outer radius of coil (mm)	40
Mixing tube diameter (mm)	1
Standoff distance (mm)	2
Pressure (MPa)	10–30
Abrasive mesh number (#)	1200
Impact angle (°)	90°
Abrasive feed rate (g/s)	0.5
Duration time of ejection (s)	0.5

Fig. 9 Depth contours of eroded craters under different conditions (pressure = 10 MPa). **a** Current = 0 A. **b** Current = 1.5 A

The results of present research indicated that MR jet has the potential for precise machining of complex shapes. The finding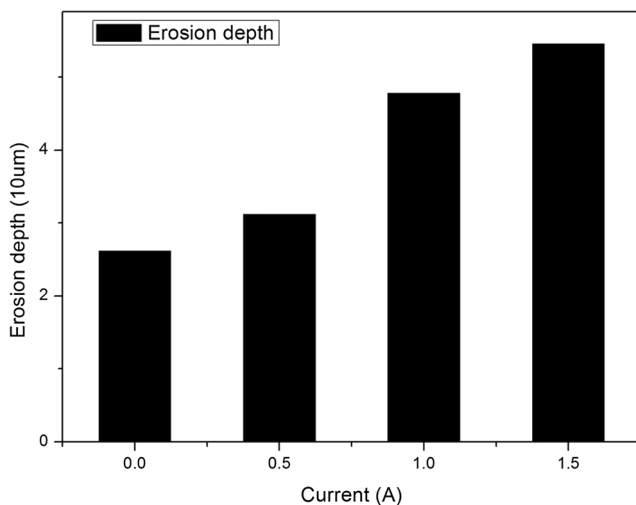s can be used as guidelines for optimizing operation parameters in practical utilization of this technique. The interaction between the particles and the MR fluid will be further studied.

Data availability Not applicable

Code availability The software used in the present study is authorized.

Declarations

Conflict of interest The authors declare that they have no conflict of interest.

Fig. 10 Erosion depths of MR jets under different currents (pressure = 10 MPa)

References

1. Zelenak M, Foldyna J, Scucka J, Hloch S, Riha Z (2015) Visualisation and measurement of high-speed pulsating and continuous water jets. Meas J Int Meas Confed 72:1–8. https://doi.org/10.1016/j.measurement.2015.04.022

2. Lv Z, Hou R, Tian Y, Huang C, Zhu H (2018) Investigation on flow field of ultrasonic-assisted abrasive waterjet using CFD with discrete phase model. Int J Adv Manuf Technol 96:963–972. https://doi.org/10.1007/s00170-018-1635-4

3. Kowsari K, Nouhi A, Hadavi V, Spelt JK, Papini M (2017) Prediction of the erosive footprint in the abrasive jet micromachining of flat and curved glass. Tribol Int 106:101–108. https://doi.org/10.1016/j.triboint.2016.10.038

4. Liu H, Wang J, Kelson N, Brown RJ (2004) A study of abrasive waterjet characteristics by CFD simulation. J Mater Process Technol 153–154:488–493. https://doi.org/10.1016/j.jmatprotec.2004.04.037

5. Hou R, Huang C, Zhu H (2014) Numerical simulation ultrahigh waterjet (WJ) flow field with the high-frequency velocity vibration at the nozzle inlet. Int J Adv Manuf Technol 71:1087–1092. https://doi.org/10.1007/s00170-013-5493-9

6. Umehara N, Kalpakjian S (1994) Magnetic fluid grinding - a new technique for finishing advanced ceramics. CIRP Ann Manuf Technol 43:185–188. https://doi.org/10.1016/S0007-8506(07)62192-1

7. Jacobs SD, Golini D, Hsu Y, Puchebner BE, Strafford D, Prokhorov IV et al (1995) Magnetorheological finishing: a deterministic process for optics manufacturing. In: Kasai T (ed) Int. Conf. Opt. Fabr. Test, vol 2576, pp 372–382. https://doi.org/10.1117/12.215617

8. Nie M, Cao J, Li J, Fu M (2019) Magnet arrangements in a magnetic field generator for magnetorheological finishing. Int J Mech Sci 161–162:105018. https://doi.org/10.1016/j.ijmecsci.2019.105018

9. Jha S (2004) Design and development of the magnetorheological abrasive flow finishing (MRAFF) process. Int J Mach Tools Manuf 44:1019–1029. https://doi.org/10.1016/j.ijmachtools.2004.03.007

10. Jha S, Jain V (2006) Modeling and simulation of surface roughness in magnetorheological abrasive flow finishing (MRAFF) process. Wear 261:856–866. https://doi.org/10.1016/j.wear.2006.01.043

11. Wang Y, Yin S, Huang H (2016) Polishing characteristics and mechanism in magnetorheological planarization using a permanent magnetic yoke with translational movement. Precis Eng 43:93–104. https://doi.org/10.1016/j.precisioneng.2015.06.014

12. Wang H, Zhang F, Zhang Y, Luan D (2007) Research on material removal of ultrasonic- magnetorheological compound finishing. Int J Mach Mach Mater 2:50–58

13. Tricard M, Kordonski WI, Shorey AB (2006) Magnetorheological jet finishing of conformal, freeform and steep concave optics. CIRP Ann Manuf Technol 55:309–312. https://doi.org/10.1016/S0007-8506(07)60423-5

14. Jayswal SC, Jain VK, Dixit PM (2005) Modeling and simulation of magnetic abrasive finishing process. Int J Adv Manuf Technol 26:477–490. https://doi.org/10.1007/s00170-004-2180-x

15. Liu JG, Wang WC (2004) Energy and helicity preserving schemes for hydro- and magnetohydro-dynamics flows with symmetry. J Comput Phys 200:8–33. https://doi.org/10.1016/j.jcp.2004.03.005

16. Lv Z, Hou R, Tian Y, Huang C, Zhu H (2018) Numerical study on flow characteristics and impact erosion in ultrasonic assisted waterjet machining. Int J Adv Manuf Technol 98:373–383. https://doi.org/10.1007/s00170-018-2271-8

17. Lv Z, Huang C, Zhu H, Wang J, Wang Y, Yao P (2015) A research on ultrasonic-assisted abrasive waterjet polishing of hard-brittle materials. Int J Adv Manuf Technol 78:1361–1369. https://doi.org/10.1007/s00170-014-6528-6

18. Lv Z, Hou R, Huang C, Zhu H, Wang J (2018) Investigation on erosion mechanism in ultrasonic assisted abrasive waterjet machining. Int J Adv Manuf Technol 94:3741–3755. https://doi.org/10.1007/s00170-017-0995-5